

RR 264



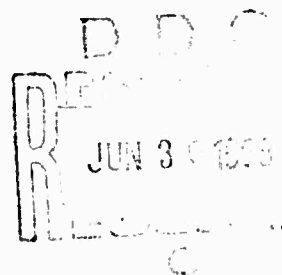
Research Report 264

THE ATTENUATION  
AND BACKSCATTERING  
OF INFRARED RADIATION  
BY ICE FOG AND WATER FOG

Motoi Kumai  
and  
Jack D. Russell

April 1969

AD 689447



U.S. ARMY MATERIEL COMMAND  
TERRESTRIAL SCIENCES CENTER  
**COLD REGIONS RESEARCH & ENGINEERING LABORATORY**  
HANOVER, NEW HAMPSHIRE

THIS DOCUMENT HAS BEEN APPROVED FOR PUBLIC RELEASE  
AND SALE; ITS DISTRIBUTION IS UNLIMITED.

Approved for  
CLEANING  
RESEARCH



Research Report 264

THE ATTENUATION  
AND BACKSCATTERING  
OF INFRARED RADIATION  
BY ICE FOG AND WATER FOG

Motoi Kumai  
and  
Jack D. Russell

April 1969

DA PROJECT 1T061101A91A  
U.S. ARMY MATERIEL COMMAND  
TERRESTRIAL SCIENCES CENTER  
**COLD REGIONS RESEARCH & ENGINEERING LABORATORY**  
HANOVER, NEW HAMPSHIRE

THIS DOCUMENT HAS BEEN APPROVED FOR PUBLIC RELEASE  
AND SALE: ITS DISTRIBUTION IS UNLIMITED.

### PREFACE

This report was prepared by Dr. Motoi Kumai, Research Physicist, Research Division, Cold Regions Research and Engineering Laboratory (CRREL), U.S. Army Terrestrial Sciences Center (USA TSC). Computer work was done by SP5 Jack D. Russell of CRREL.

The report covers the optical and physical studies of ice fog undertaken by CRREL as a FY68 ILIR project with partial support from the U.S. Army Arctic Test Center. This report was published under DA Project 1T061101A91A, *In-House Laboratory Independent Research*.

USA TSC is a research activity of the Army Materiel Command.

## CONTENTS

	Page
Preface.....	ii
Abstract.....	iv
Introduction.....	1
Physical properties of ice fog.....	1
Mie scattering computations.....	4
Results.....	5
Literature cited.....	7

## ILLUSTRATIONS

Figure	
1. Ice fog crystals formed at -39C ambient temperature .....	2
2. Size and mass distribution of ice-fog crystals formed at -39C ambient temperature .....	2
3. Size and mass distribution of ice-fog crystals formed at -41C ambient temperature .....	3

## TABLES

Table	
I. Physical properties of ice fog at Fairbanks, Alaska .....	3
II. Optical constants of ice and water .....	5
III. The attenuation coefficients $b(m^{-1})$ .....	6
IV. The backscattering functions $\beta(\pi)(m^{-1}sr^{-1})$ .....	6

#### ABSTRACT

Ice-fog crystals consisting of many spherical particles, and some hexagonal plates and columns, were observed at ambient temperatures of about  $-40^{\circ}\text{C}$  in the Fairbanks, Alaska, area during mid-winter. The concentrations and the size distributions of the ice-fog crystals were measured. The attenuation and backscattering of infrared radiation by ice-fog crystals were computed for optical wavelengths of  $2.2\mu$ ,  $2.7\mu$ ,  $4.5\mu$ ,  $5.75\mu$ ,  $9.7\mu$  and  $10.9\mu$  using the Mie theory. The minimum attenuation coefficients and backscattering functions of ice fog were found to be at  $9.7\mu$  wavelength in the observed wavelengths. Optical attenuation coefficients and volume backscattering functions of water fogs were also computed using the Mie theory. The minimum attenuation coefficients and backscattering functions of water fog were found to be at  $10.9\mu$  wavelength in the region of  $2.2\mu$ ,  $2.7\mu$ ,  $4.5\mu$ ,  $5.75\mu$ ,  $9.7\mu$  and  $10.9\mu$ . Both the attenuation coefficients and backscattering functions of ice fog are within the same order of magnitude as water fog for equivalent fog concentrations and wavelengths.

# **THE ATTENUATION AND BACKSCATTERING OF INFRARED RADIATION BY ICE FOG AND WATER FOG**

by

Motoi Kumai and Jack D. Russell

## **INTRODUCTION**

By reducing visibility, ice fog hampers the normal flow of traffic during severe cold weather conditions in subarctic countries. In addition, ice fog can cause extinction of the infrared beam in an infrared guidance system. Because of this, the emphasis of CRREL's ice fog research is being placed on the effects of ice fog on infrared transmission. This report presents results of a study of attenuation and backscattering of infrared radiation by fog in Alaska.

## **PHYSICAL PROPERTIES OF ICE FOG**

The physical properties of ice fog in the Fairbanks, Alaska, area have been studied by Thuman and Robinson (1954). The formation of ice fog and its nuclei have been studied by Kumai (1964) and Kumai and O'Brien (1965).

The optical properties of fog depend on the number concentration and size distribution of the particles, which can vary significantly during different meteorological conditions. Establishing a representative fog model is not an easy task. Determination of the collection efficiency for fog droplets with radii approaching the wavelength of near-infrared radiation is one of the problems in fog sampling.

Ice-fog crystals and ice crystals are initial stages in the formation of snow crystals. Because their sizes and optical properties are quite different, it is convenient to consider them separately. Ice crystals have well-formed hexagonal plates and columns. They are often called "diamond dust" because of the way they twinkle under a low sun or under nighttime illumination. Ice crystals form at about  $-25^{\circ}\text{C}$  and are  $20\mu$  to  $300\mu$  in diameter. They have much lower concentrations and do not affect visibility as adversely as ice fog does. Ice-fog crystals consist of many spherical particles, equant crystals with rudimentary faces, and some hexagonal plates and columns of  $2\mu$  to  $30\mu$  diameter formed at ambient temperatures of about  $-40^{\circ}\text{C}$  by spontaneous nucleation (Fig. 1).

Ice-fog distributions at air temperatures of  $-39^{\circ}\text{C}$  and  $-41^{\circ}\text{C}$  in the Fairbanks, Alaska, area are shown in Figure 2 and Figure 3. The number of particles and the mass of fog per unit volume are shown as a function of crystal diameter. Table 1 summarizes the important physical properties of each fog spectrum.



Figure 1. Ice fog crystals formed at  $-39^{\circ}\text{C}$  ambient temperature.

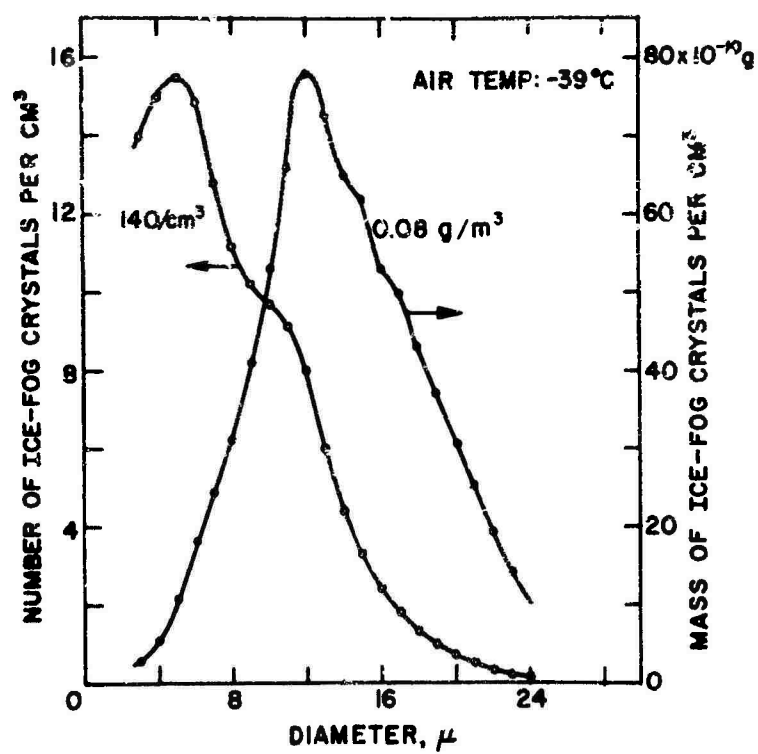


Figure 2. Size and mass distribution of ice-fog crystals formed at  $-39^{\circ}\text{C}$  ambient temperature.

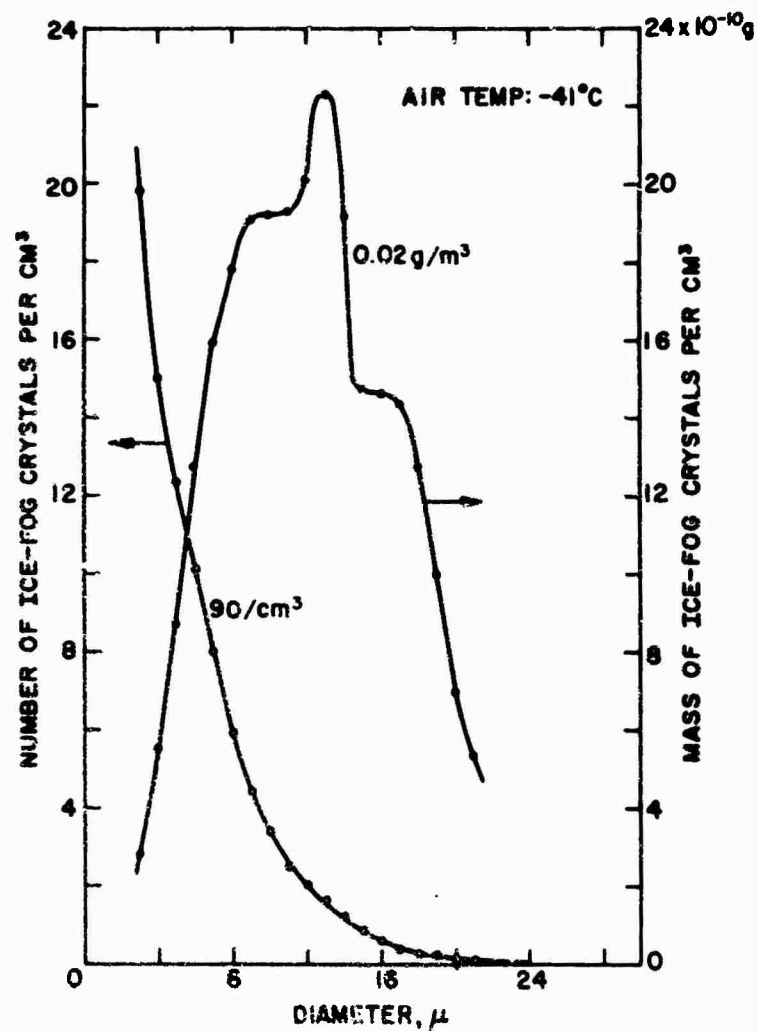


Figure 3. Size and mass distribution of ice-fog crystals formed at  $-41^{\circ}\text{C}$  ambient temperature.

Table I. Physical properties of ice fog at Fairbanks, Alaska.

Observations	$N$ (no./cm <sup>3</sup> )	$r_{\text{mode}}$ (μ)	$r_{\text{min}}$ (μ)	$r_{\text{max}}$ (μ)	$\Delta r$ (μ)	Air temp ( $^{\circ}\text{C}$ )	L.W.C. (g/m <sup>3</sup> )
No. 1 (Fig. 2)	140	3.0	1.5	12.0	0.5	-39	0.08
No. 2 (Fig. 3)	90	1.5	1.5	12.0	0.5	-41	0.02

$N$  = total concentration

$r_{\text{mode}}$  = mode radius = radius corresponding to the maximum number of ice-fog crystals

$r_{\text{min}}$  = minimum radius

$r_{\text{max}}$  = maximum radius

$\Delta r$  = radius interval containing  $n(r)$  crystals, where  $N = \sum_r n(r)$

L.W.C. = liquid water content.



## MIE SCATTERING COMPUTATIONS

The Mie theory is an exact solution of Maxwell's electromagnetic theory for spheres; it describes the field inside and outside a sphere for any scattering angle, size, and index of refraction.

For backscattering, the scattering angle equals  $\pi$  radians. The particle size parameter is  $x = k'a$  where  $k' = 2\pi/\lambda$ ,  $a$  is the radius of the spheres, and  $\lambda$  is the wavelength of incident radiation.

When dealing with actual particles, scattering due to the sphere's dielectric properties alone is not sufficient to define fully the intensity of the backscattered radiation; the contribution due to absorption within the sphere must also be included. This requires a complex index of refraction of the form  $m = n - ik$ , where  $m = (\epsilon - 4\pi\sigma/\omega)^{1/2}$ ,  $\epsilon$  being the dielectric constant,  $\sigma$  the conductivity, and  $\omega$  the angular frequency of the electromagnetic wave.

The computational method as outlined in Carrier et al. (1967) appears quite simple at first glance. In the present study we are interested in the attenuation coefficient due to scattering,  $b$ , and the volume backscattering function,  $\beta(\pi)$ . The quantity  $b$  is the coefficient in the relationship

$$I = I_0 \exp(-bf) \quad (1)$$

defining the decrease in light intensity while passing through a medium of length  $f$ .

According to the above-mentioned paper,

$$b = \sum_{r_{\min}}^{r_{\max}} n(r) \delta r \pi^2 K_{\text{ext}}(x, m) \text{ [meter}^{-1}\text{]} \quad (2)$$

and

$$\beta(\pi) = \frac{\lambda^2}{4\pi^2} \sum_{r_{\min}}^{r_{\max}} n(r) \delta r i_1(\pi, x, m) \quad (3)$$

where  $n(r)$  is the number of particles per unit volume per  $\delta r$  radius interval,  $K_{\text{ext}}$  is the total extinction cross section of one particle, and  $i_1$  is the Mie intensity function of a scattered component whose electric vector is either perpendicular or parallel to the plane of observation. When  $\theta = \pi$ , then  $i_1 = i_2$ .

The problem becomes more difficult, however, when we examine the work by Deirmendjian and Clasen (1962), which outlines a computational scheme to derive values for  $K_{\text{ext}}$  and  $i_1$ . The method involves the use of ordinary Bessel functions, and circular and hyperbolic functions with complex argument. Although the functions may be reduced to fairly simple recursion formulas, the presence of complex quantities in the denominator of most of the terms requires long and tedious algebraic manipulation to make the problem programmable. It must also be kept in mind that a computer deals with pure numbers and that the real and the imaginary parts of a complex number must be dealt with individually.

The greatest consumer of computer real-time is the evaluation of the recursion formulas which consist of very slowly converging infinite series. It is not unusual to find that 300-350 terms are required to solve for just one value of the quantities  $K_{\text{ext}}$  and  $i_1$ , of which there are as many values as there are radius intervals. We must then multiply the number of radius intervals by the number of wavelengths in question when estimating total run-time.

In Figures 2 and 3, the radius interval,  $\Delta r$ , is  $0.5\mu$ . Particle concentrations for each fog radius  $n(r_k)$  were punched on paper tape for subsequent entry into the computer. Computer calculations of the attenuation coefficient and backscattering functions from eq 2 and 3 were made for the fog size distributions of Figure 2 and Figure 3, using the optical constants of ice by Kislovskii (1959) and the optical constants of water by Centeno (1941).

The recent investigations on the optical properties of ice were done by Hornig *et al.* (1958), Ockman (1958), and Zander (1966). However, their papers do not present the values of the refractive index ( $n$ ) and extinction coefficient ( $k$ ) of ice. Due to the experimental difficulties, our present knowledge of the optical constants of ice in the infrared region is inexact compared with our knowledge of those of water. The optical constants of ice and water used for this computer calculation are presented in Table II (Centeno, 1941; Kislovskii, 1959).

Table II. Optical constants of ice and water.

Wavelength in microns $\lambda$	Ice		Water	
	Extinction coefficient $k$	Refraction index $n$	Extinction coefficient $k$	Refraction index $n$
2.2	0.0005	1.29	0.0005	1.293
2.7	0.03	1.19	0.0183	1.216
4.5	0.01	1.33	0.0164	1.341
5.75	0.01	1.24	0.0427	1.273
9.7	0.08	1.13	0.0579	1.230
10.9	0.20	1.12	0.0993	1.150

## RESULTS

Optical attenuation coefficients and volume backscattering functions were computed for the observed Alaskan ice fogs for optical wavelengths of  $2.2\mu$ ,  $2.7\mu$ ,  $4.5\mu$ ,  $5.75\mu$ ,  $9.7\mu$  and  $10.9\mu$  using the Mie theory. The calculations were made for ice-fog crystal concentrations of 70, 140, 280 and  $420/\text{cm}^3$  with size distribution shown in Figure 2; and ice-fog crystal concentrations of 90, 180, 270 and  $360/\text{cm}^3$  with size distribution shown in Figure 3. The attenuation coefficients  $b(\text{m}^{-1})$  and the backscattering functions  $\beta(\pi)(\text{m}^{-1}\text{sr}^{-1})$  of ice-fog crystals are presented in Tables III and IV. The minimum attenuation coefficient and backscattering function are found to be at  $9.7\mu$  wavelength for the computed wavelength range of  $2.2\mu$ ,  $2.7\mu$ ,  $4.5\mu$ ,  $5.75\mu$ ,  $9.7\mu$  and  $10.9\mu$ . The optical wavelengths of  $2.2\mu$ ,  $9.7\mu$  and  $10.9\mu$  are those corresponding to atmospheric windows. The wavelengths of  $2.7\mu$  and  $4.5\mu$  fall within the absorption bands of both water vapor and carbon dioxide, and the wavelength of  $5.75\mu$  is within the absorption band of water vapor.

When the air temperatures were above  $-15^\circ\text{C}$ , supercooled fogs were observed in the Fairbanks, Alaska, area during mid-winter. Optical attenuation coefficients and volume backscattering functions of water fogs were computed for optical wavelengths of  $2.2\mu$ ,  $2.7\mu$ ,  $4.5\mu$ ,  $5.75\mu$ ,  $9.7\mu$  and  $10.9\mu$  using the Mie theory. The calculations were done for fog-droplet concentrations of 70, 140, 280 and  $420/\text{cm}^3$  with size distributions shown in Figure 2, and fog-droplet concentrations of 90, 180, 270 and  $360/\text{cm}^3$  with size distributions shown in Figure 3. The attenuation coefficients  $b(\text{m}^{-1})$  and the backscattering functions  $\beta(\pi)(\text{m}^{-1}\text{sr}^{-1})$  of water fogs are presented in Tables III and IV. Both the attenuation coefficients and backscattering functions of ice fog and water fog are within the same order of magnitude for the same fog concentrations and wavelengths. The

Table III. The attenuation coefficients  $k(m^{-1})$ .

Size distribution of fog droplets	Concentration of fog droplets no./cm <sup>3</sup>	Liquid water content g/m <sup>3</sup>	Wavelength, $\mu$					
			2.2	2.7	4.5	5.75	9.7	10.9
Ice-fog								
Fig. 2	70	0.089	$1.153 \times 10^{-2}$	$1.212 \times 10^{-2}$	$1.321 \times 10^{-2}$	$1.304 \times 10^{-2}$	$5.130 \times 10^{-3}$	$6.795 \times 10^{-3}$
Fig. 2	140	0.077	$2.306 \times 10^{-2}$	$2.424 \times 10^{-2}$	$2.642 \times 10^{-2}$	$2.606 \times 10^{-2}$	$1.026 \times 10^{-2}$	$1.359 \times 10^{-2}$
Fig. 2	280	0.15	$4.611 \times 10^{-2}$	$4.848 \times 10^{-2}$	$5.283 \times 10^{-2}$	$5.216 \times 10^{-2}$	$2.052 \times 10^{-2}$	$2.717 \times 10^{-2}$
Fig. 2	420	0.23	$6.917 \times 10^{-2}$	$7.272 \times 10^{-2}$	$7.925 \times 10^{-2}$	$7.824 \times 10^{-2}$	$3.078 \times 10^{-2}$	$4.076 \times 10^{-2}$
Fig. 2	90	0.023	$6.932 \times 10^{-3}$	$6.694 \times 10^{-3}$	$9.719 \times 10^{-3}$	$7.939 \times 10^{-3}$	$3.046 \times 10^{-3}$	$4.206 \times 10^{-3}$
Fig. 3	180	0.047	$1.786 \times 10^{-2}$	$1.789 \times 10^{-2}$	$1.944 \times 10^{-2}$	$1.588 \times 10^{-2}$	$6.092 \times 10^{-3}$	$8.616 \times 10^{-3}$
Fig. 3	270	0.070	$2.680 \times 10^{-2}$	$2.608 \times 10^{-2}$	$2.916 \times 10^{-2}$	$2.382 \times 10^{-2}$	$9.138 \times 10^{-3}$	$1.292 \times 10^{-2}$
Fig. 3	360	0.093	$3.573 \times 10^{-2}$	$3.478 \times 10^{-2}$	$3.883 \times 10^{-2}$	$3.176 \times 10^{-2}$	$1.218 \times 10^{-2}$	$1.723 \times 10^{-2}$
Water-fog								
Fig. 2	70	0.089	$1.153 \times 10^{-2}$	$1.217 \times 10^{-2}$	$1.314 \times 10^{-2}$	$1.282 \times 10^{-2}$	$7.846 \times 10^{-3}$	$5.455 \times 10^{-3}$
Fig. 2	140	0.077	$2.306 \times 10^{-2}$	$2.434 \times 10^{-2}$	$2.626 \times 10^{-2}$	$2.564 \times 10^{-2}$	$1.568 \times 10^{-2}$	$1.091 \times 10^{-2}$
Fig. 2	280	0.15	$4.611 \times 10^{-2}$	$4.868 \times 10^{-2}$	$5.256 \times 10^{-2}$	$5.127 \times 10^{-2}$	$3.137 \times 10^{-2}$	$2.182 \times 10^{-2}$
Fig. 2	420	0.23	$6.916 \times 10^{-2}$	$7.308 \times 10^{-2}$	$7.883 \times 10^{-2}$	$7.691 \times 10^{-2}$	$4.705 \times 10^{-2}$	$3.273 \times 10^{-2}$
Fig. 3	90	0.023	$6.919 \times 10^{-3}$	$9.054 \times 10^{-3}$	$9.675 \times 10^{-3}$	$8.256 \times 10^{-3}$	$4.504 \times 10^{-3}$	$3.256 \times 10^{-3}$
Fig. 3	180	0.047	$1.784 \times 10^{-2}$	$1.811 \times 10^{-2}$	$1.935 \times 10^{-2}$	$1.651 \times 10^{-2}$	$9.008 \times 10^{-3}$	$6.509 \times 10^{-3}$
Fig. 3	270	0.070	$2.673 \times 10^{-2}$	$2.716 \times 10^{-2}$	$2.902 \times 10^{-2}$	$2.477 \times 10^{-2}$	$1.351 \times 10^{-2}$	$9.764 \times 10^{-3}$
Fig. 3	360	0.093	$3.568 \times 10^{-2}$	$3.622 \times 10^{-2}$	$3.870 \times 10^{-2}$	$3.303 \times 10^{-2}$	$1.802 \times 10^{-2}$	$1.302 \times 10^{-2}$

Table IV. The backscattering functions  $\beta(m^{-1}sr^{-1})$ .

Size distribution	Concentration of fog droplets no./cm <sup>3</sup>	Liquid water content g/m <sup>3</sup>	Wavelength, $\mu$					
			2.2	2.7	4.5	5.75	9.7	10.9
Ice-fog								
Fig. 2	70	0.089	$4.804 \times 10^{-6}$	$9.134 \times 10^{-6}$	$1.251 \times 10^{-5}$	$2.695 \times 10^{-5}$	$2.764 \times 10^{-5}$	$5.450 \times 10^{-5}$
Fig. 2	140	0.077	$9.609 \times 10^{-6}$	$1.827 \times 10^{-5}$	$2.501 \times 10^{-5}$	$5.389 \times 10^{-5}$	$5.927 \times 10^{-5}$	$1.090 \times 10^{-4}$
Fig. 2	280	0.15	$1.922 \times 10^{-5}$	$3.654 \times 10^{-5}$	$5.002 \times 10^{-5}$	$1.078 \times 10^{-4}$	$1.185 \times 10^{-4}$	$2.180 \times 10^{-4}$
Fig. 2	420	0.23	$2.888 \times 10^{-5}$	$5.481 \times 10^{-5}$	$7.502 \times 10^{-5}$	$7.502 \times 10^{-5}$	$1.778 \times 10^{-4}$	$3.271 \times 10^{-4}$
Fig. 3	90	0.023	$2.744 \times 10^{-6}$	$5.794 \times 10^{-6}$	$7.515 \times 10^{-6}$	$1.936 \times 10^{-5}$	$2.485 \times 10^{-5}$	$4.589 \times 10^{-5}$
Fig. 3	180	0.047	$5.489 \times 10^{-6}$	$1.159 \times 10^{-5}$	$1.503 \times 10^{-5}$	$3.872 \times 10^{-5}$	$4.970 \times 10^{-5}$	$9.179 \times 10^{-5}$
Fig. 3	270	0.070	$8.238 \times 10^{-6}$	$1.786 \times 10^{-5}$	$2.255 \times 10^{-5}$	$5.938 \times 10^{-5}$	$7.455 \times 10^{-5}$	$1.377 \times 10^{-4}$
Fig. 3	360	0.093	$1.098 \times 10^{-5}$	$2.318 \times 10^{-5}$	$3.006 \times 10^{-5}$	$7.745 \times 10^{-5}$	$9.940 \times 10^{-5}$	$1.886 \times 10^{-4}$
Water-fog								
Fig. 2	70	0.039	$9.60 \times 10^{-6}$	$2.699 \times 10^{-5}$	$9.409 \times 10^{-5}$	$1.535 \times 10^{-4}$	$1.170 \times 10^{-4}$	$4.103 \times 10^{-4}$
Fig. 2	140	0.077	$9.960 \times 10^{-6}$	$5.397 \times 10^{-5}$	$1.887 \times 10^{-4}$	$3.070 \times 10^{-4}$	$2.339 \times 10^{-4}$	$8.206 \times 10^{-4}$
Fig. 2	280	0.15	$1.992 \times 10^{-5}$	$1.079 \times 10^{-4}$	$3.760 \times 10^{-4}$	$8.181 \times 10^{-4}$	$4.679 \times 10^{-4}$	$1.641 \times 10^{-3}$
Fig. 2	420	0.23	$2.988 \times 10^{-5}$	$1.819 \times 10^{-4}$	$5.840 \times 10^{-4}$	$9.271 \times 10^{-4}$	$7.018 \times 10^{-4}$	$2.462 \times 10^{-3}$
Fig. 3	90	0.023	$2.878 \times 10^{-6}$	$1.673 \times 10^{-5}$	$5.990 \times 10^{-5}$	$1.816 \times 10^{-4}$	$8.933 \times 10^{-5}$	$8.465 \times 10^{-4}$
Fig. 3	180	0.047	$5.745 \times 10^{-6}$	$3.346 \times 10^{-5}$	$1.198 \times 10^{-4}$	$2.632 \times 10^{-4}$	$1.783 \times 10^{-4}$	$6.931 \times 10^{-4}$
Fig. 3	270	0.070	$8.618 \times 10^{-6}$	$5.019 \times 10^{-5}$	$1.796 \times 10^{-4}$	$3.948 \times 10^{-4}$	$2.680 \times 10^{-4}$	$1.040 \times 10^{-3}$
Fig. 3	360	0.093	$1.149 \times 10^{-5}$	$6.892 \times 10^{-5}$	$2.395 \times 10^{-4}$	$5.265 \times 10^{-4}$	$3.573 \times 10^{-4}$	$1.386 \times 10^{-3}$

minimum attenuation coefficient and backscattering functions of water fog were found to be at  $10.9\mu$  wavelength for the observed wavelengths of  $2.2\mu$ ,  $2.7\mu$ ,  $4.5\mu$ ,  $5.75\mu$ ,  $9.7\mu$ , and  $10.9\mu$ .

These calculations describe only the effect of water droplets and ice crystals on the attenuation and scattering of radiation. For computations of total attenuation and scattering, the effects of the atmospheric absorption bands, especially water vapor and  $\text{CO}_2$ , would also have to be considered.

#### LITERATURE CITED

- Carner, L.W., Cato, G.A. and von Essen, K.J. (1967) The backscattering and extinction of visible and infrared radiation by selected major cloud models. *Applied Optics*, vol. 6, p. 1209.
- Centeno, M. (1941) The refractive index of liquid water in the near infra-red spectrum. *Journal of the Optical Society of America*, vol. 31, p. 244.
- Deirmendjian, D. and Clasen, R.J. (1962) Light scattering of partially absorbing homogeneous spheres of finite size. The Rand Corporation, Report R-393-PR.
- Hornig, D.F., White, H.F. and Reding, F.P. (1958) The infrared spectra of crystalline  $\text{H}_2\text{O}$ ,  $\text{D}_2\text{O}$ , and  $\text{HDO}$ . *Spectrochimica Acta.*, vol. 12, p. 338.
- Kislovskii, L.D. (1959) Optical characteristics of water and ice in the infrared and radiowave regions of the spectrum. *Optika i Spektroskopiia*, vol. 7, p. 311.
- Kumai, M. (1964) A study of ice fog and ice-fog nuclei at Fairbanks, Alaska. U.S. Army Cold Regions Research and Engineering Laboratory (USA CRREL) Research Report 150, Part I.
- and O'Brien (1965) A study of ice fog and ice-fog nuclei at Fairbanks, Alaska. USA CRREL Research Report 150, Part II.
- Ockman, N. (1958) The infrared and Raman spectra of ice. *Advances in Physics*, vol. 7, p. 199.
- Thuman, W.C. and Robinson, E. (1954) Studies of Alaskan ice-fog particles. *Journal of Meteorology*, vol. 16, p. 151-156.
- Zander, R. (1966) Spectral scattering properties of ice clouds and hoarfrost. *Journal of Geophysical Research*, vol. 71, p. 375-378.

Unclassified  
Security Classification

DOCUMENT CONTROL DATA - R & D		
<small>(Security classification of title, body of abstract and indexing annotation must be entered when the overall report is classified)</small>		
1. ORIGINATING ACTIVITY (Corporate author) Cold Regions Research and Engineering Laboratory U.S. Army Terrestrial Sciences Center, Hanover, New Hampshire 03755		2a. REPORT SECURITY CLASSIFICATION Unclassified
		2b. GROUP
3. REPORT TITLE THE ATTENUATION AND BACKSCATTERING OF INFRARED RADIATION BY ICE FOG AND WATER FOG		
4. DESCRIPTIVE NOTES (Type of report and inclusive dates) Research Report		
5. AUTHOR(S) (Print name, middle initial, last name) Motoi Kumai and Jack D. Russell		
6. REPORT DATE April 1969	7a. TOTAL NO. OF PAGES 11	7b. NO. OF REFS 10
8a. CONTRACT OR GRANT NO. b. PROJECT NO. DA Project 1T061101A91A c. d.	9a. ORIGINATOR'S REPORT NUMBER(S) Research Report 264 9b. OTHER REPORT NUM(S) (Any other numbers that may be assigned this report)	
10. DISTRIBUTION STATEMENT This document has been approved for public release and sale; its distribution is unlimited.		
11. SUPPLEMENTARY NOTES Partial support from: U.S. Army Arctic Test Center Ft. Greely, Alaska		12. SPONSORING MILITARY ACTIVITY Cold Regions Research & Engineering Laboratory, U.S. Army Terrestrial Sciences Center, Hanover, New Hamp- shire 03755
13. ABSTRACT Ice-fog crystals consisting of many spherical particles, and some hexagonal plates and columns, were observed at ambient temperatures of about -40C in the Fairbanks, Alaska, area during mid-winter. The concentrations and the size distributions of the ice-fog crystals were measured. The attenuation and backscattering of infrared radiation by ice-fog crystals were computed for optical wavelengths of 2.2 $\mu$ , 2.7 $\mu$ , 4.5 $\mu$ , 5.75 $\mu$ , 9.7 $\mu$ and 10.9 $\mu$ using the Mie theory. The minimum attenuation coeff- icients and backscattering functions of ice fog were found to be at 9.7 $\mu$ wavelength in the observed wavelengths. Optical attenuation coefficients and volume backscat- tering functions of water fogs were also computed using the Mie theory. The mini- mum attenuation coefficients and backscattering functions of water fog were found to be at 10.9 $\mu$ wavelength in the region of 2.2 $\mu$ , 2.7 $\mu$ , 4.5 $\mu$ , 5.75 $\mu$ , 9.7 $\mu$ and 10.9 $\mu$ . Both the attenuation coefficients and backscattering functions of ice fog are within the same order of magnitude as water fog for equivalent fog concentrations and wavelengths.		
14. Key Words Ice fog Infrared Alaska - meteorology		

DD FORM 1473  
1 NOV 66

REPLACES DD FORM 1473, 1 JAN 64, WHICH IS  
OBSOLETE FOR ARMY USE.

Unclassified

Security Classification